Interlayer tunnelling mechanism: experimental test of single layer compounds

A. A. Tsvetkov[a,b], D. van der Marel[a], D. Dulic[a],
H. J. Molegraaf[a], N. N. Kolesnikov[c], B. Willemsen[d], and Z. F. Ren[e]

[a]Material Science Center, Laboratory of Solid State Physics,
University of Groningen, Nijenborgh 4, 9747 AG Groningen, The Netherlands

[b]Department of Solid State Physics, P. N. Lebedev Physical Institute
Russian Academy of Sciences, Leninsky Prospect 53, 117924 Moscow, Russia

[c]Institute of Solid State Physics, Russian Academy of Sciences, Chernogolovka 142432, Russia

[d]Superconductor Technologies, 460 Ward Drive, Santa Barbara CA 93111-2310, USA

[e]Department of Chemistry, SUNY at Buffalo, Buffalo NY 14260-3000, USA

ABSTRACT

The c-axis optical properties of cuprate superconductors have been studied by grazing angle reflectivity technique. We tested the interlayer tunnelling (ILT) model of high temperature superconductivity and showed that the basic relation between the condensation energy of the superconducting state and the interlayer Josephson coupling does not hold for $Tl_2Ba_2CuO_6$. Measuring the reflectivity at an oblique angle of incidence on the ab-surface of $Tl_2Ba_2CuO_6$, we found the c-axis plasma resonance at 28 cm^{-1}. The corresponding Josephson coupling energy is at least an order of magnitude lower than the condensation energy determined from the specific heat measurements. In the double layer compound $Tl_2Ba_2CaCu_2O_8$ the c-axis plasma resonance was observed at 26 cm^{-1}. The c-axis penetration depth and the c-axis conductivity follow the Ambegaokar-Baratoff or "dirty limit" superconductor relation if a very small energy gap is assumed.

Keywords: Josephson plasmon, interlayer tunnelling model

1. INTRODUCTION

The remarkably strong anisotropy of high-T_c superconductors puts forward the question whether the superconductivity is a two dimensional or three dimensional phenomenon, and how the anisotropy relates to the mechanism of superconductivity. Physical properties characteristic of both 2D and 3D systems can be observed in the normal state; moreover, the dimensionality of some compounds can be changed with doping.[1] The high-T_c cuprates are often considered to be a stack of conducting CuO_2 planes separated by insulating or poorly conducting intermediate layers, which play the role of carrier doping reservoirs for CuO_2. The optical response in the ab-plane has a metallic nature with a well defined plasma edge around 1 eV or higher. In contrast, the c-axis spectra of most high-T_c's are similar to those of ionic insulators with sharp phonon features and no Drude peak in optical conductivity. In Fig. 1a, the optical conductivity of $La_{2-x}Sr_xCuO_4$ is shown for light polarized along the a-axis and the c-axis. The ab-plane optical conductivity of LSCO has a Drude like peak, as one can see from the upper part of the figure. The c-axis conductivity is almost flat at far infrared frequencies. Its absolute value is below the Mott limit and more than two orders of magnitude lower than the in-plane conductivity. For these reasons, transport along the c-axis is considered to be incoherent.

However, the superconducting state reveals more three-dimensional character. As can be seen from Fig. 1a, a part of the spectral weight below the energy gap is shifted into the delta-function at zero frequency in the superconducting state, which corresponds to the formation of a superconducting condensate. The reduction of conductivity occurs for both polarizations. This leads to the recovery of coherent transport along the c-axis. Due to the low value of the out-of plane conductivity, the spectral weight transferred into the delta-function is very small. The corresponding

Send correspondence to A. A. Tsvetkov. E-mail: tsvetkov@phys.rug.nl

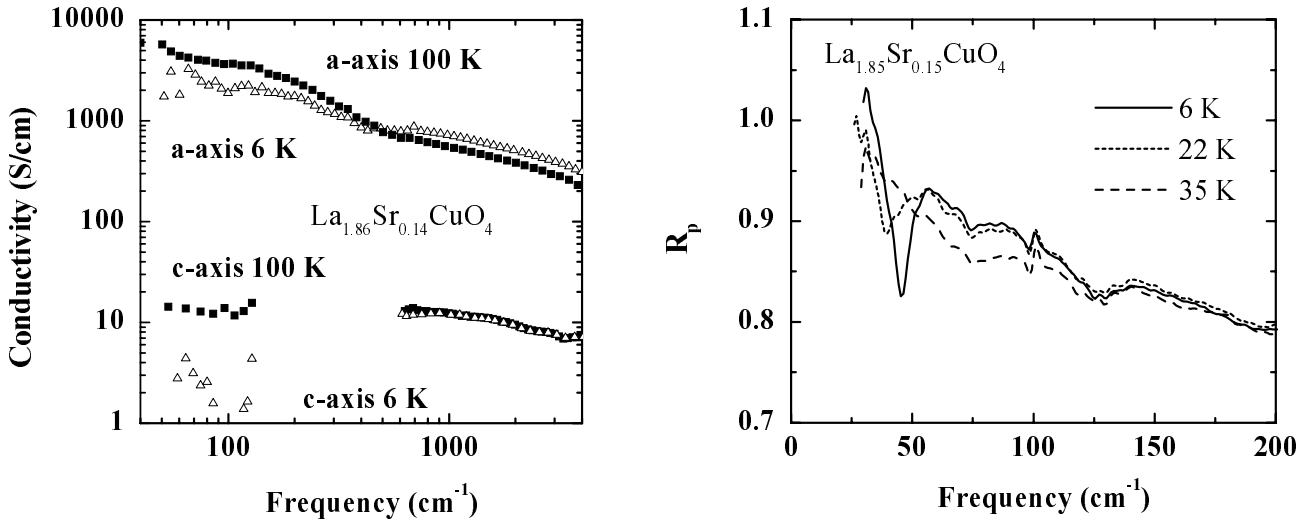

Figure 1. a) Optical conductivity of $La_{1.86}Sr_{0.14}CuO_4$ for light polarized along the a-axis (upper part) and c-axis (lower part) at 100 K (solid squares) and 6 K (open triangles). For simplicity, the phonon frequency range is removed from the c-axis conductivity plot, b) reflectivity R_p of $La_{1.86}Sr_{0.14}CuO_4$ single crystal measured with p-polarized light incident on the ab surface at an angle of 80^o.

plasma frequency lies well below the superconducting energy gap, and the plasma oscillations along the c-axis are not damped. This results in the development of a c-axis plasma resonance in the superconducting state, similar to that seen at 50 cm^{-1} in grazing angle spectra of $La_{1.85}Sr_{0.15}CuO_4$ shown in Fig. 1b. The appearance of the sharp plasma edge in the superconducting state has been reported for $La_{2-x}Sr_xCuO_4$[2] and $YBa_2Cu_3O_x$[3] for different levels of doping. Because of the strong anisotropy of critical current density and penetration depth, the superconductivity is believed to occur in the CuO_2 planes, which are coupled to each other by the Josephson effect. The electrodynamical properties in this case are described by the Lawrence-Doniach model.[4]

An alternative model in which superconductivity is driven by pair tunneling has been proposed by Anderson.[5] The interlayer tunneling (ILT) model postulates that single electron motion along the c-axis is prohibited due to charge-spin separation. This confinement of electrons within CuO_2 planes raises their kinetic energy with respect to the free interplane motion. In the superconducting state, pairs can tunnel between the planes, which stabilizes the superconductivity. According to the ILT model[6–8] the major contribution to the condensation energy E_{cond} results from the Josephson energy of interlayer coupling E_J[4]

$$\hbar^2\omega_{pc}^2 = 4\pi d a^{-2}(2e)^2 E_J\,, \tag{1}$$

where ω_{pc} is the c-axis plasma frequency, d is the distance between the CuO_2 planes, a is the in-plane lattice parameter, $\hbar$ is the Planck constant, and e is the electron charge.

The key prediction of the ILT model, $E_{cond} \equiv E_J$ provides an opportunity for a direct test. Both quantities E_{cond} and E_J can be measured experimentally. Unambiguous comparison between the theory and experiment is possible for compounds with equally spaced CuO_2 planes and a high transition temperature, such as $Tl_2Ba_2CuO_6$ or $HgBa_2CuO_4$. The Josephson energy is obtained from infrared measurements of the plasma frequency according to Eq. 1. Alternatively, the c-axis plasma frequency can be calculated from the c-axis penetration depth λ_c according $\omega_{pc} = c/\lambda_c$, where c is the speed of light. The condensation energy is determined from the temperature dependence of the electronic specific heat. The main reason for testing the ILT model on single layer compounds as opposed to bilayer or multilayer compounds, is to exclude possible interference of the Josephson coupling of the CuO_2 planes across the unit cell with that within the same unit cell. In a layered system with alternating Josephson interactions, the weaker coupling determines the out-of-plane penetration depth or the plasma frequency, while the stronger coupling sets the transition temperature.

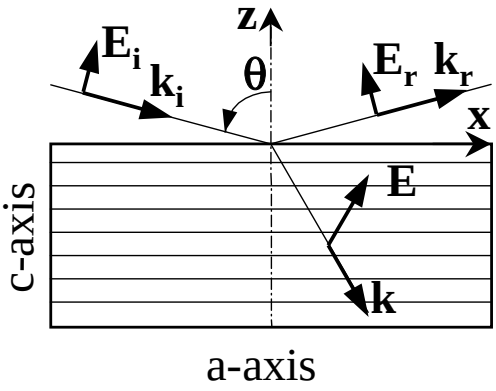

Figure 2. Layout of the grazing angle reflectivity technique.

In this paper we review the measurements of the c-axis plasma frequency for $Tl_2Ba_2CuO_6$ and $Tl_2Ba_2CaCu_2O_8$. Due to the absence of samples with a large ac-plane dimension, the optical measurements were done by the grazing angle reflectivity technique, which is discussed below. We argue that the c-axis plasma frequency is too small to account for the high transition temperature in this compound, which is in variance with the ILT model. At the end we discuss interlayer transport in $Tl_2Ba_2CuO_6$ in comparison with the other high temperature superconductors.

2. GRAZING ANGLE TECHNIQUE

Let us consider the interaction of an electromagnetic plane wave polarized in the plane of incidence, with anisotropic media. Quite generally, high-T_c superconductors can be treated as uniaxial crystals, with properties described by dielectric functions $\varepsilon_{ab}(\omega)$ and $\varepsilon_c(\omega)$. The reflectivity R_p from the *ab*-surface in vacuum is given by the Fresnel formula, which can be presented in the following way:

$$R_p = \left| \frac{\sqrt{\varepsilon_{ab}}\cos\theta - \sqrt{1 - \frac{\sin^2\theta}{\varepsilon_c}}}{\sqrt{\varepsilon_{ab}}\cos\theta + \sqrt{1 - \frac{\sin^2\theta}{\varepsilon_c}}} \right|^2 , \tag{2}$$

where θ is an angle of incidence. The layout for the grazing angle measurements is shown in Fig. 2. From equation 2 one can see that R_p has a singularity if $\varepsilon_c(\omega)$ is equal to zero, i. e. at the c-axis longitudinal frequencies; otherwise, the reflectivity is mainly determined by the in-plane complex refractive index $\tilde{n}(\omega) = \sqrt{\varepsilon_{ab}(\omega)}$ and the angle of incidence. To emphasize this we can calculate a function,[8] which is directly obtained from measured reflectivity R_p:

$$L(\omega) = \frac{(1 - R_p)|n_{ab}|\cos\theta}{2(1 + R_p)} \sim \mathrm{Im} e^{i\phi}\sqrt{1 - (\sin^2\theta/\varepsilon_c)} , \tag{3}$$

where n_{ab} is the in-plane complex refraction index and $\phi = \pi/2 - \arg n_{ab}$ is a weakly frequency dependent phase shift. We call it a pseudo-loss function because it has maxima at the same frequencies as the loss-function $\mathrm{Im}(-1/\varepsilon_c)$. In order to understand why R_p is sensitive to the longitudinal modes we need to consider the dielectric tensor of an anisotropic superconductor.

The incident electromagnetic radiation excites a wave inside the material, which has electric field component $\vec{\tilde{\mathbf{E}}} = \vec{\mathbf{E}} e^{i(\vec{\mathbf{k}}\vec{\mathbf{r}} - \omega t)}$, where each component of $\vec{\mathbf{E}}$ and $\vec{\mathbf{k}}$ can be complex. If the x-axis lies at the intersection of the plane of incidence and the surface, and the z-axis is normal to the surface, then the x-component of the wave vector, k_x, is determined by the incident radiation, while the z-component of the wave vector can be shown to depend on both in-plane and out-of-plane dielectric functions, as follows:

$$k_x = \frac{\omega}{c}\sin\theta, \qquad\qquad k_z^2 = \frac{\omega^2}{c^2}\varepsilon_{ab}\left(1 - \frac{\sin^2\theta}{\varepsilon_c}\right) , \tag{4}$$

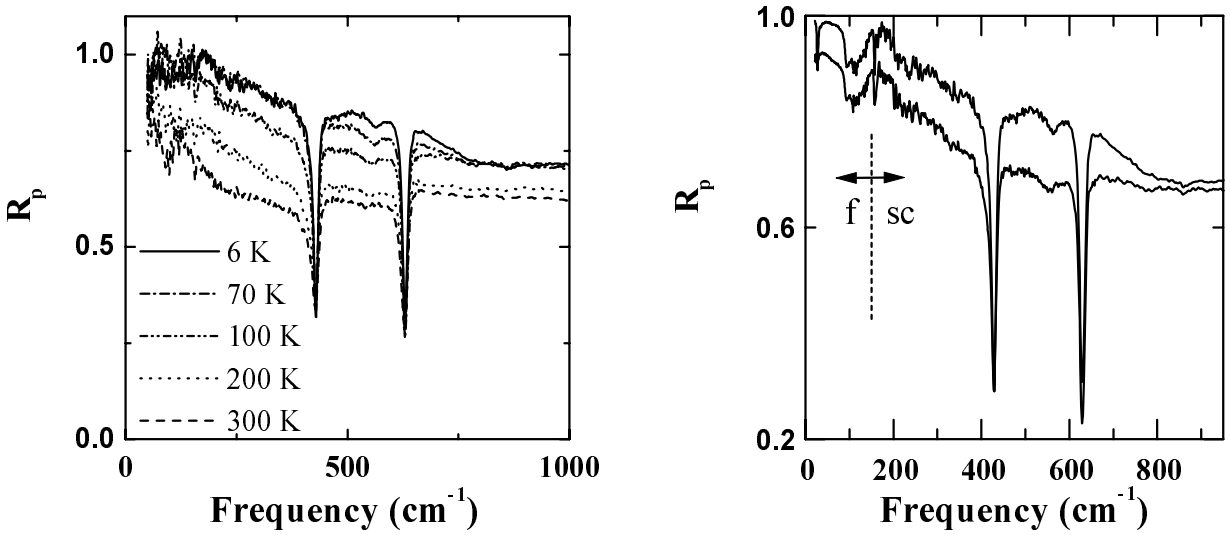

Figure 3. a) Reflectivity R_p of $Tl_2Ba_2CuO_6$ single crystal measured with p-polarized light incident on the ab surface at an angle of 80^o for different temperatures, b) reflectivity R_p of $Tl_2Ba_2CuO_6$ single crystal from (a) and film together for 6 K (upper curve) and 100 K (lower curve). The dashed line separate the single crystal and the film data.

where ω is the frequency of incident radiation and c is the speed of light. Inside the media the wave remains polarized in the xz-plane, and the components of electric field relate to each other as:

$$\frac{E_z}{E_x} = \frac{\sqrt{\varepsilon_{ab}}}{\sqrt{\varepsilon_c - \sin^2\theta}}\,. \tag{5}$$

This illustrates the well known fact that the electromagnetic wave in an anisotropic media does not have a pure transverse character, but it also has a longitudinal component, unless it propagates along the principal axes.

In most high-T_c compounds the c-axis plasma frequency is far below phonon frequencies, while the in-plane response is mostly dominated by plasma oscillations of carriers in the ab-plane. Thus, the dielectric functions at very low frequencies can be written in both cases as a pure plasma response:

$$\varepsilon_{ab}(\omega) = \varepsilon_\infty^{ab} - \frac{\omega_{pab}^2}{\omega^2}, \qquad\qquad \varepsilon_c(\omega) = \varepsilon_{sc} - \frac{\omega_{pc}^2}{\omega^2}\,, \tag{6}$$

where ω_{pab} and ω_{pc} are the in-plane and out-of-plane plasma frequencies, respectively, and ε_{sc} includes also the phonon response.

Substitution of Eqs. 6 into Eqs. 4 gives a pure imaginary solution for k_z everywhere, except for a narrow frequency range between $\omega_{pc}/\sqrt{\varepsilon_{sc}}$ and $\omega_{pc}/\sqrt{\varepsilon_{sc} - \sin^2\theta}$. In this region k_z is real and also strongly frequency dependent. This corresponds to the propagation of the electromagnetic wave in the media. Outside of this region the electromagnetic wave decays exponentially near the surface, which gives rise to total reflection.

In optical measurements the screened plasma frequency $\omega_{pc}/\sqrt{\varepsilon_{sc}}$ is determined, as can be seen from Eqs. 6. The screening of the media ε_{sc} can be obtained after subtraction of free carrier response from the total dielectric function

$$\varepsilon_c(\omega) = \varepsilon_\infty^c - \frac{\omega_{pc}^2}{\omega^2} + \frac{4\pi i\sigma_c}{\omega} + \sum_j \frac{S_j\omega_j^2}{\omega_j^2 - \omega^2 - i\omega\gamma_j}\,, \tag{7}$$

where the first term represents high energy interband transitions, the second and the third terms are superconducting and normal carrier responses, respectively, and the last is the sum of phonon contribution.

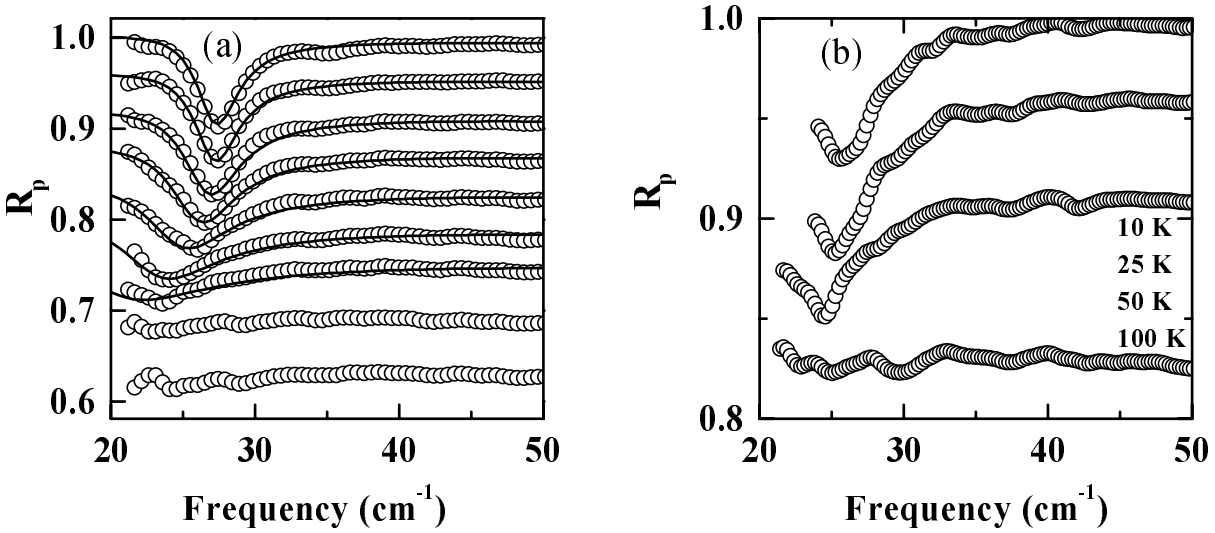

Figure 4. a) p-polarized reflectivity R_p of $Tl_2Ba_2CuO_6$ film at 6, 10, 20, 30, 40, 50, 60, 75, and 90 K with light incident on the ab surface at 80^o (open circles) and a simulation (solid line) as described in the text. The curves are shifted by 3%. b) Reflectivity R_p of $Tl_2Ba_2CaCu_2O_8$ film in the same geometry. The curves have the offset of 4% with respect to each other.

3. C-AXIS PLASMA FREQUENCY

Because of the higher transition temperature and larger interlayer distance, $Tl_2Ba_2CuO_6$ should have its Josephson resonance at a higher frequency than that of $La_{2-x}Sr_xCuO_4$. Measurements performed on high quality single crystals did not reveal any plasma edge in the FIR and MIR region.[9] The reflectivity R_p of $Tl_2Ba_2CuO_6$ at 80^o angle of incidence for p-polarization is shown in Fig. 3a. R_p is seen to increase gradually as temperature decreases, following the reflectivity in the ab-plane. The three deep minima at 143, 451, and 648 cm^{-1}, which correspond to the longitudinal phonon frequencies, do not show any substantial temperature dependence. Because in the normal state the free-carrier response is known to be overdamped, the appearance of an undamped plasma oscillations in the superconducting state would result in the dramatic changes in the spectrum. No sharp plasma feature resembling those of $La_{1.85}Sr_{0.15}CuO_4$ in Fig. 1b could be observed in the whole measured region. From those measurements an upper limit on the c-axis plasma frequency was set to 100 cm^{-1}.

At low frequencies the diffraction scattering of light limits the measurements. Due to the lack of large single crystals an oriented film was used at the lower frequencies in order to overcome the diffraction limit. In grazing angle measurements the in-plane conductivity determines the penetration depth and thus, a thin film can be used to study c-axis optical properties. Shown in Fig. 3b are two reflectivity spectra for 100 K and 6 K from Fig. 3a together with two spectra obtained on a $Tl_2Ba_2CuO_6$ film. An appearance of a sharp dip at very low frequency can be seen in the 6 K curve, which is absent in the 100 K data. The single crystal curves and film curves match each other in the overlapping region. This fact together with the close transition temperatures, $T_c = 80$ and 82 K for the film and the crystal, respectively, imply a similar doping level.

In Fig. 4a the dependence of the grazing angle reflectivity for the $Tl_2Ba_2CuO_6$ film at frequencies below 50 cm^{-1} is shown for different temperatures. The curves are shifted by 3% for clarity. A clear resonance feature is seen at 27.8 cm^{-1} in the 6 K spectrum.[10] As the temperature is increased the resonance moves to lower frequencies and above 70 K it shifts out of the measurement range. The temperature dependence of the resonance frequency $\omega(T)^2/\omega(6K)^2$ is shown in Fig. 5b. The width of the absorption line is very small, and the corresponding oscillations are almost undamped. We ascribed this resonance to the Josephson plasmon, a collective oscillations of the superfluid condensate along the c-axis.

Fig. 5a shows the reflectivity spectra of another sample. The second film is more transparent. The Josephson plasmon is observed at the same frequency as in the first film. In addition, a strong temperature dependent soft

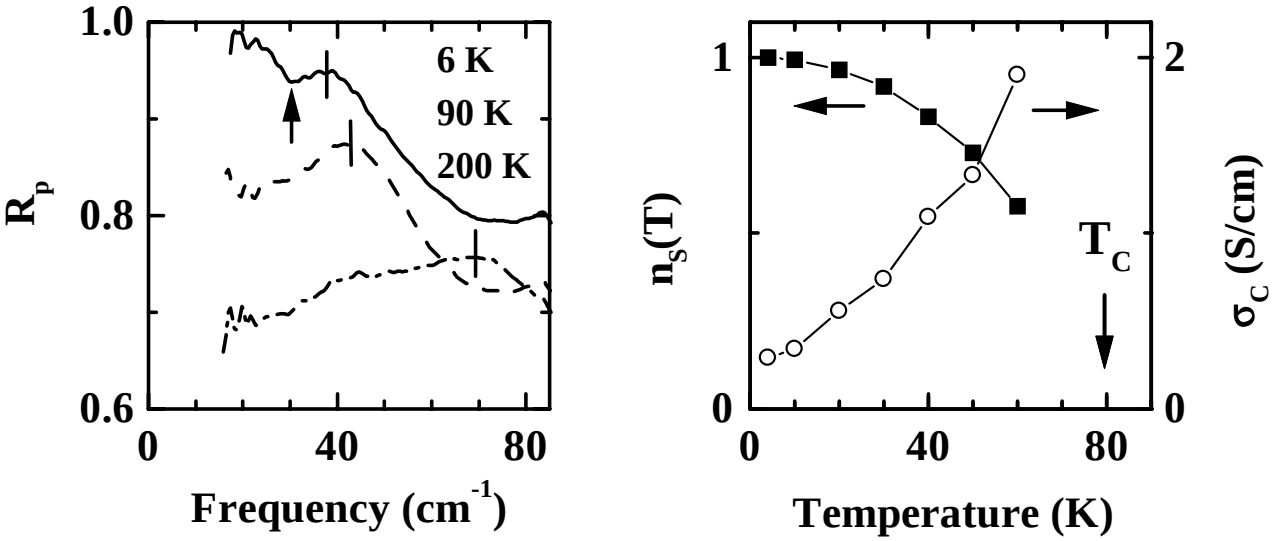

Figure 5. a) Reflectivity R_p of a transparent $Tl_2Ba_2CuO_6$ film with light incident at 80^o for 6, 90, and 200 K. Vertical lines mark the shift of a soft mode of the substrate $SrTiO_3$. The c-axis plasma edge is shown with arrow, b) temperature dependencies of $n_s(T) = \omega_{pc}(T)^2/\omega_{pc}(6K)^2$ and optical conductivity $\sigma_c(T)$ at $\omega_{pc}(T)$.

phonon mode originating from the $SrTiO_3$ substrate is present in the spectra. Although the optical properties of $SrTiO_3$ are well studied, even the most recent measurements[11] do not provide data on IR active modes at such low frequencies. In order to exclude the possibility that the minimum around 30 cm^{-1} originated from the substrate, we performed measurements on the $SrTiO_3$ substrate in the same geometry. In these measurements - data are not shown - the appearance of extra phonon modes below the phase transition at 110 K was observed at higher frequencies, and the soft mode responsible for the hump in Fig. 5a followed the temperature dependence reported in Ref. 11, but no additional structure in the range of interest was seen.

The double layer compound $Tl_2Ba_2CaCu_2O_8$, which has a higher superconducting transition temperature, reveals a similar or even lower c-axis plasma frequency. The reflectivity spectra are shown in Fig. 4. The plasma minimum occurs at 26 cm^{-1} for 10 K and follow a temperature shift similar to the single layer compound.

For a purely electronic system the Josephson resonance frequency $\omega_{pc} = c/\lambda_c$ is determined by the supercurrent density of states along the c-axis. In the present case the Josephson plasma resonance is located at a frequency below the infrared active lattice vibrations. The corresponding dynamical electric field is screened by the ion polarization and the lattice vibrations, characterized by a dielectric constant ε_{sc}. As a result, the Josephson resonance is actually observed at the reduced frequency $\omega_J = \varepsilon_{sc}^{-1/2} c/\lambda_c$. After performing a complete optical analysis of these spectra in the frequency range from 20 to 6000 cm^{-1} using Fresnel's equations for reflection from anisotropic optical media at oblique angle of incidence, the dielectric function ε_{cs} can be extracted from these data. For frequencies below 40 cm^{-1}, $\varepsilon_{cs} = 11.3 \pm 0.5$ and therefor $\lambda_c(6K) = 17.0 \pm 0.3\mu$m or $\omega_p c = 93.5$ cm^{-1}.

The c-axis penetration depth in many high-T_c materials can be measured directly by scanning squid microscopy. The imaging of the Josephson interlayer vortices in $Tl_2Ba_2CuO_6$ single crystal gave the value $\lambda_c(4K) = 17 \pm 4\mu$m.[10,12] Squid microscopy can overestimate the penetration depth, because vortices are generally pinned to spots with weaker superconductivity. Nevertheless, this is excellent agreement between the optical and squid data.

The temperature dependence of the plasma frequency and c-axis conductivity can be extracted from the reflectivity spectra in Fig. 4a, using Eqs. 2 and 7. For $T < T_c$ and frequencies below the gap and the phonon frequencies, Eq. 7 can be reduced to $\varepsilon_{ab}(\omega) = -c^2/\lambda_a^2\omega^2$ and $\varepsilon_c(\omega) = \varepsilon_{sc} + 4\pi i\sigma_c/\omega - c^2/\lambda_c^2\omega^2$. The first and the second terms for $\varepsilon_c(\omega)$ are conserved, because we are measuring close to the c-axis plasma resonance. The width of the resonance is determined by $\sigma_c(\omega)$.[8] The spectra in Fig. 4a were fitted using λ_a, λ_c, and σ_c as fitting parameters. The temperature dependencies of $\lambda_c(6K)^2/\lambda_c(T)^2$ and σ_c are shown in Fig. 5b. The optical conductivity decreases with temperature, as the spectral weight is transferred to the zero frequency.

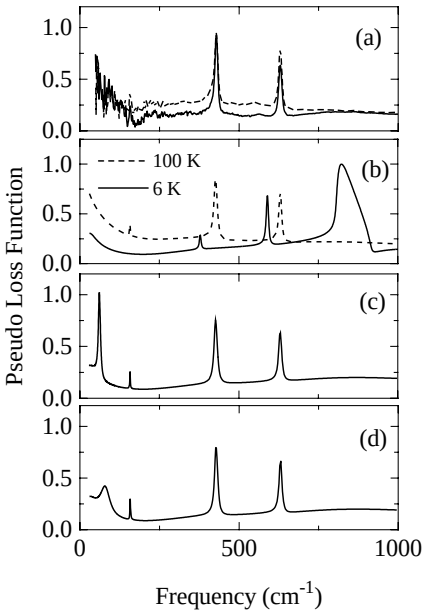

Figure 6. Pseudo-loss function $L(\omega)$ for $Tl_2Ba_2CuO_6$: (a) experimental data at 6 (solid line) and 100 K (dashed), (b) simulation for the normal state (dashed), simulation for the superconducting state (solid lines) with (b) ILT value $\omega_{pc} = 1500$ cm^{-1} and $\sigma_c(\omega_{pc}) = 0.5$ S/sm, (c) $\omega_{pc} = 200$ cm^{-1} and $\sigma_c(\omega_{pc}) = 0.5$ S/sm, (d) $\omega_{pc} = 200$ cm^{-1} and $\sigma_c(\omega_{pc}) = 3$ S/sm.

4. DISCUSSION

4.1. Interlayer tunneling model

Using Eq. 1 we calculate the plasma frequency, predicted by ILT model. For $Tl_2Ba_2CuO_6$ the ILT value of unscreened plasma frequency is $\omega_{pc} = 1500$ cm^{-1},[9] which is far above the observed value. To provide a direct comparison of the ILT theory with experiment, we display in Fig. 6a the c-axis pseudo-loss function $L(\omega)$ for $Tl_2Ba_2CuO_6$ in the normal and in the supercondcting state. To first approximation, $L(\omega) \sim 1 - R_p$. For comparison, the pseudo-loss functions is shown for $\omega_{pc} = 1500$ cm^{-1} in Fig. 6b and for $\omega_{pc} = 200$ cm^{-1} with $\sigma_c = 3$ S/cm and $\sigma_c = 0.5$ S/cm in Fig. 6 (c) and (d), respectively.[9] In case of the ILT value a sharp plasma maximum appears at the screened plasma frequency and the phonon frequencies are shifted dramatically. This picture does not correlate with the experimental spectra. For a lower value the plasma resonance occurs below the phonon range and no phonon frequency renormalization is seen. The height and the width of plasma peak depend strongly on the c-axis conductivity.

The ILT model demands an equality of condensation energy E_{cond} to the Josephson energy. We can calculate which part the Josephson tunneling contributes to E_{cond}. Leggett[7] introduced the parameter $\eta = E_J/E_{cond}$. For the case of $Tl_2Ba_2CuO_6$ the condensation energy can be determined from the specific heat measurements of Loram *et al*,[13] $E_{cond} = 100 \pm 20\mu$eV per formula unit. Using Eq. 1 with the following parameters $d = 11.6$ Å and $a = 3.87$ Å, we can calculate the Josephson energy $E_J = 0.24\mu$eV per unit formula $Tl_2Ba_2CuO_6$. Thus, the contribution due to the Josephson tunneling is only $\eta = E_J/E_{cond} = 0.24 \pm 0.05\%$, and we can conclude that the gain in the condensation energy due to the reduction of kinetic energy of pairs in the superconducting state is negligible.

The observation of the Josephson plasma resonance in $Tl_2Ba_2CaCu_2O_8$ provides an additional argument against the ILT model, because electrons are not confined any more within one layer. The close values of plasma frequencies in single and double layer compounds imply that the coupling within the double layer CuO_2 is much stronger than between them, and that the plasma frequency is determined by the properties of a single Josephson junction across the intermediate layers.

4.2. Interplane conductivity

Recently, Basov *et al.*[14] found a correlation between the c-axis penetration depth and interplane conductivity $\lambda_c^2\sigma_n =$ const. This can be interpreted it two ways. In the case of dirty limit BCS superconductors the relation is given by the Glover-Tinkham-Ferrel sum rule[15]

$$\lambda_c^2\sigma_n = \hbar c^2/4\pi^2\Delta\tanh(\Delta/2k_BT)\,, \tag{8}$$

where k_B is Boltzmann's constant and Δ is the superconducting energy gap. If layered cuprates are considered as a stack of superconducting planes coupled by the Josephson effect, the c-axis penetration depth is determined by the critical current density according to the Lawrence-Doniach theory $c^2/\lambda_c^2 = 8\pi edJ_c/\hbar$, where d is the distance between planes and J_c is the c-axis critical current density. In the case of BCS superconductors J_c is determined by the Ambegaokar-Baratoff relation $J_c = \pi\Delta(T)\sigma_n\tanh(\Delta(T)/2k_BT)/2ed$, which eventually results in Eq. 8. A direct observation of Josephson current between the layers[16] makes the second approach more favorable. However, with finite tunneling probability between the layers one can expect the formation of narrow bands, which in turn results in coherent motion along the c-axis and a metallic temperature dependence of the resistivity. This is not the case for many high-T_c superconductors, except for optimally doped $YBa_2Cu_3O_x$. The coherency between the planes is effectively removed by the high in-plane scattering. Indeed, the tunneling rate can be evaluated as $\Gamma_T = \hbar/\tau_T = \hbar a^2\sigma_c/2e^2dN(E_F)$, where a is the in-plane lattice constant, $N(E_F)$ is the density of states at the Fermi level. The density of states for $Tl_2Ba_2CuO_6$ can be estimated from specific heat data,[13] $N(E_F) \approx 1.4$ states/eV per Cu-atom. Thus, $\Gamma_T \approx 0.3$ cm^{-1} is much smaller than the in-plane scattering rate, which is of the order of 100 cm^{-1}.

In order to compare data for $Tl_2Ba_2CuO_6$ with the dependence of Basov *et al.*,[14] we used the Ambegaokar-Baratoff relation to estimate the "missing area" in the optical conductivity, which is proportional to $\Delta_T\,\delta\sigma_c$, where Δ_T is the energy gap measured by tunneling spectroscopy[17] ($\Delta_T \approx 22$ meV), and $\delta\sigma_c$ is the effective conductivity transfered to the δ-function in $\sigma_c(\omega)$. This way, we obtained $\delta\sigma_c = 0.26$ S/cm, which is an order of magnitude smaller than the experimental DC conductivity $\sigma_c = 2$ S/cm in the normal state just above T_C. This small value of $\delta\sigma_c$ correlates with those of $La_{2-x}Sr_xCuO_4$[18] and underdoped $YBa_2Cu_3O_x$.[14] A possible explanation for such a low value of σ_{AB} is that a part of carriers responsible for high optical conductivity does not contribute to the superconducting condensate, as it was reported for the in-plane response of $Tl_2Ba_2CuO_6$,[19] and consequently, it reduces the c-axis plasma frequency.

5. SUMMARY

The c-axis response of $Tl_2Ba_2CuO_6$ was studied by grazing angle reflectivity measurements. In the superconducting state the Josephson plasma oscillation was observed at 27.8 cm^{-1}. The corresponding Josephson energy was found to contribute no more than 0.24% to the condensation energy of the superconducting state, which contradicts the predictions of the interlayer tunneling model, where the superconductivity is the result of the Josephson interlayer coupling. The correlation between the c-axis penetration depth and the c-axis conductivity found recently by Basov *et al.*[14] for many high temperature superconductors seems to hold for $Tl_2Ba_2CuO_6$ also.

ACKNOWLEDGMENTS

One of us (A.A.T) acknowledges the support by the Nederlandse Organisatie voor Wetenschappelijk Onderzoek (NWO), the Russian Superconductivity Program under project #96-120 and RFBR under project #97-02-17593.

REFERENCES

1. S. L. Cooper and K. E. Gray, "Anisotropy and interlayer coupling in the high T_c cuprates," in *Physical Properties of High Temperature Superconductors IV*, D. M. Ginsberg, ed., pp. 61–188, World Scientific Publishing Co. Pte. Ltd., Singapore, 1994.
2. K. Tamasaku, Y. Nakamura, and S. Uchida, "Charge dynamics across the CuO_2 planes in $La_{2-x}Sr_xCuO_4$," *Phys. Rev. Lett.* **69**, pp. 1455–1458, 1992.
3. C. C. Homes, T. Timusk, R. Liang, D. A. Bonn, and W. N. Hardy, "Optical conductivity of c axis oriented $YBa_2Cu_3O_{6.70}$: evidence for a pseudogap," *Phys. Rev. Lett.* **71**, pp. 1645–1648, 1993.

4. W. E. Lawrence and S. Doniach, "The theory of layer structure superconductors," in *Proceedings of the 12th International Conference on Low Temperature Physics*, E. Kando, ed., pp. 361–362, Academic Press, Kyoto, Japan, 1971.
5. P. W. Anderson, *The Theory of Superconductivity in the High-T_c Cuprates*, University Press, Princeton, NJ, 1997.
6. P. W. Anderson, "Interlayer tunnelling mechanism for high-T_c superconductivity: comparison with c axis infrared experiments," *Science* **268**, pp. 1154–1155, 1995.
7. A. J. Leggett, "Interlayer tunnelling models: implications of a recent experiment," *Science* **274**, pp. 587–590, 1996.
8. D. van der Marel, J. Schützmann, H. Somal, and J. W. van der Eb, "Electrodynamical properties of high T_c superconductors studied with polarized angle resolved infrared spectroscopy," in *Proceedings of the 10th anniversary HTS workshop on physics, materials and applications*, B. Batlogg, C. W. Chu, W. K. Chu, D. U. Gubser, and K. A. Müller, eds., pp. 357–370, World Scientific Publishing Co. Pte. Ltd., Singapore, 1996.
9. J. Schützmann, H. S. Somal, A. A. Tsvetkov, D. van der Marel, G. E. J. Koops, N. Koleshnikov, Z. F. Ren, J. H. Wang, E. Brück, and A. A. Menovsky, "Experimental test of the interlayer pairing model for high-T_c superconductivity using grazing-incidence infrared reflectometry," *Phys. Rev. B* **55**, pp. 11118–11121, 1997.
10. A. A. Tsvetkov, D. van der Marel, K. A. Moler, J. R. Kirtley, J. L. de Boer, A. Meetsma, Z. F. Ren, N. Koleshnikov, D. Dulic, A. Damascelli, M. Grüninger, J. Schützmann, J. W. van der Eb, H. S. Somal, and J. H. Wang, "Global and local measures of the intrinsic josephson coupling in $Tl_2Ba_2CuO_6$," *Nature* , in press, 1998.
11. K. Kamarás, K.-L. Barth, F. Keilmann, R. Henn, M. Reedyk, C. Thomsen, M. Cardona, J. Kircher, and P. L. Richards, "The low-temperature infrared optical functions of $SrTiO_3$ determined by reflectance spectroscopy and spectroscopic ellipsometry," *J. Appl. Phys.* **78**, pp. 1235–1240, 1995.
12. K. A. Moler, J. R. Kirtley, D. G. Hinks, T. W. Li, and M. Xu, "Images of interlayer josephson vortices in $Tl_2Ba_2CuO_{6+\delta}$," *Science* **279**, pp. 1193–1195, 1998.
13. J. W. Loram, K. A. Mirza, J. M. Wade, J. R. Cooper, and W. Y. Liang, "The electronic specific heat of cuprate superconductors," *Physica C* **235-240**, pp. 134–137, 1994.
14. D. N. Basov, T. Timusk, B. Dabrowski, and J. D. Jorgensen, "c-axis response of $YBa_2Cu_4O_8$: a pseudogap and possibility of josephson coupling of CuO_2 planes," *Phys. Rev. B* **50**, pp. 3511–3514, 1994.
15. M. Tinkham, *Introduction to Superconductivity*, McGraw-Hill, New York, 1975.
16. R. Kleiner, F. Steinmeyer, G. Kunkel, and P. Müller, "Intrinsic josephson effect in $Bi_2Sr_2CaCu_2O_8$ single crystals," *Phys. Rev. Lett.* **68**, pp. 2394–2397, 1992.
17. L. Ozyuzer, Z. Yusof, J. F. Zasadzinski, R. Mogilevsky, D. G. Hinks, and K. E. Gray, "Evidence of $d_{x^2-y^2}$ symmetry in the tunneling conductance density of states of $Tl_2Ba_2CuO_6$," *Phys. Rev. B* **57**, pp. 3245–3248, 1998.
18. S. Uchida and K. Tamasaku, "Josephson plasma in the c-axis optical spectrum of high-T_c superconductors," *Physica C* **293**, pp. 1–7, 1997.
19. A. V. Puchkov, T. Timusk, S. Doyle, and A. M. Hermann, "ab-plane optical properties of $Tl_2Ba_2CuO_{6+\delta}$," *Phys. Rev. B* **51**, pp. 3312–3315, 1995.